Silicon Nitride Nanopillars and Nanocones Formed by Nickel Nanoclusters and Inductively Coupled Plasma Etching for Solar Cell Application

2009 Jpn. J. Appl. Phys. 48 126508

(http://iopscience.iop.org/1347-4065/48/12R/126508)

Japanese Journal of Applied Physics **48** (2009) 126508 **REGULAR PAPER**

Silicon Nitride Nanopillars and Nanocones Formed by Nickel Nanoclusters and Inductively Coupled Plasma Etching for Solar Cell Application

Kartika Chandra Sahoo, Men-Ku Lin[1], Edward-Yi Chang*, Tran Binh Tinh, Yiming Li[2], and Jin-Hua Huang[1]

Department of Materials Science and Engineering, National Chiao-Tung University, Hsinchu 300, Taiwan
[1] *Department of Materials Science and Engineering, National Hsing-Hua University, Hsinchu 300, Taiwan*
[2] *Department of Electrical Engineering, National Chiao-Tung University, Hsinchu 300, Taiwan*

Received July 21, 2009; revised September 12, 2009; accepted September 17, 2009; published online December 21, 2009

The external quantum efficiency of solar cells can be improved by using textured surface with minimum reflection. We have fabricated nanopillars and nanocone structures on silicon nitride surface by means of self-assembled nickel nano particle masks with single step inductively coupled plasma (ICP) ion etching and double step ICP etching, respectively. Thus, sub-wavelength nanopillar and nanocone-like structures displaying low reflectance were obtained readily without the need for any lithography equipment. The formation mechanism of nanopillar and nanocone like structures fabricated on silicon nitride surface has been discussed. The relationship of etching time with structure height and average reflectance spectra has been drawn.

DOI: 10.1143/JJAP.48.126508

1. Introduction

The antireflection coating is a key factor for solar cell design.[1–3] Many studies have been reported for double layer antireflection (DLAR) coating because single layer antireflection (SLAR) and coatings are not able to cover a broad range of the solar spectrum. Unfortunately, these multilayer antireflection coatings (ARCs) are expensive to fabricate owing to the stringent requirements of high vacuum, material selection, and layer thickness control. A well-known way to multilayer ARCs is the sub-wavelength structure (SWS) surface with dimensions smaller than the wavelength of light.[4–8] Recently, texturization on silicon nitride (Si_3N_4) and its optical properties for solar cells has been reported using reactive ion etching (RIE) process.[9] Also the numerical study of optical properties of silicon nitride sub-wavelength structures has been studied.[10] The main motivation behind this lied in the fact that the sub-wavelength structures would act as a second ARC layer with an effective refractive index so that the total structure could perform as a DLAR layer. Thus the cost of the deposition of second ARC layer can be saved with better or comparable performance as that of a DLAR solar cell. Nevertheless, the surface profile of a sub-wavelength structure is strongly dependent on the conditions of the RIE process.[11]

In this study, we have studied the effect of RIE conditions on the profile of fabricated sub-wavelength structure on Silicon nitride antireflection coating layers. We have fabricated the silicon nitride nanopillar and nanocone structures using the self assembled nickel nanoclusters followed by inductively coupled plasma (ICP) etching on silicon substrate and explore the reflection properties of the texturing structures through spectroscopic measurements. Basically, we have explained the fabrication of nanopillars and nanocones on silicon nitride using one step and two step ICP etching methods, respectively for the first time and compared the reflection properties of the texturing structures with different morphologies.

2. Experiment

First of all the polished (100) silicon was cleaned with dilute HF to remove the native oxide. A layer of 300 nm thick silicon nitride (Si_3N_4) was then deposited on a polished (100) silicon wafer by plasma enhanced chemical vapor deposition (PECVD) technique. A nickel film with a thickness of 5 nm was then evaporated on the silicon nitride surface using an E-beam evaporating system. The nickel film was then rapid thermal annealed (RTA) under the forming gas (mixture of H_2 and N_2) with a flow rate of 3 sccm at 850 °C for 60 s to form nickelclusters, which served as the etch masks for silicon nitride. It has been observed that the diameter of Ni nano clusters decreases when the thickness of the deposited nickel film varied from 20 nm to 3 nm at 850 °C for 60 s. So we have chosen initial nickel thickness as the main parameter by keeping RTA condition constant to control the diameter of the Ni nano cluster and the initial nickel thickness of 5 nm has been chosen to get the higher density and smaller dimension of Ni nano-clusters in our experiment. The sample was then etched by ICP etcher (ULVAC NE 550) using different gases and etching parameters which will be discussed in results and discussion section. To remove the residual nickel mask, the sample was dipped into pure nitric acid (HNO_3) solution for 5 min at room temperature. The morphology of SWS was analyzed by Scanning electron micrograph (SEM). The reflectances of the SWS were measured using an N&K 1280 analyzer.

3. Results and Discussion

Figure 1 shows the schematic illustrations of the fabrication of nanopillars and nanocones by one- and two-step ICP etching processes, respectively. The one-step etching process, which is shown in Fig. 1(a), involved non-etching of nickel nanoclusters, whereas etching of the underlying silicon nitride film. As the size of the nickel nanoclusters was not changed, the etched area of the underlying silicon nitride depends on the diameter of the nano clusters. Thus, silicon nitride pillar structures were readily obtained from the one-step etching process. The two-step etching process as shown in Fig. 1(b) involved minifying of nickel nano clusters and etching of the underlying silicon nitride film, gradually. As the size of the nano clusters decreased gradually, the etched area of the underlying silicon nitride increased gradually. Thus, silicon nitride pillar structures were readily obtained from the two-step etching process. One-step etching process was carried out by using a mixture of CF_4 and O_2 and based on fluorine chemistry. The two-step

---

*E-mail address: edc@mail.nctu.edu.tw

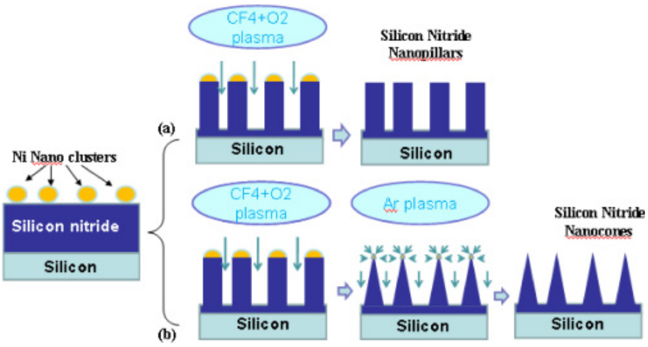

Fig. 1. (Color online) Schematic of fabrication process of (a) silicon nitride nanopillars (b) silicon nitride nanocones.

etching process was carried out by using a mixture of CF_4 and O_2 in first step and followed by the etching with Ar. The mechanism can be confirmed by watching the scanning electron microscope (SEM) image as shown in Fig. 2. The SEM image of the sample etched by Ar gas for 30 s and 120 s were shown in Figs. 2(a) and 2(b), respectively, after the nanoclusters were formed. From these figures we could see the decrease of nickel nano cluster size after etched in Ar gas for long time, which confirms the mechanism involved to form nanocones described previously. Similarly, we could see the effect of ICP etching using the mixture of CF_4/O_2 gas to form the nanopillars from the Figs. 2(c) and 2(d).

Using the developed method, experiments were performed to demonstrate control over nanopillar and nanocone height and structures. In the first series, samples starting with nickel nano clusters were etched by a gas mixture of CF_4/O_2 to between 100 to 250 nm heights by different etching time. The resulting nanopillars with corresponding heights could be seen in Figs. 3(a)–3(d). Figure 3(a) showed nanopillars with height around 110 nm with CF_4/O_2 etching time of 90 s. silicon nitride nanopillars with height around 150 nm has been achieved after etched for 120 s as shown in Fig. 3(b). Similarly, Figs. 3(c) and 3(d) showed the achieved silicon nitride nanopillars with height around 210 and 240 nm for etching time of 150 s and 180 s, respectively.

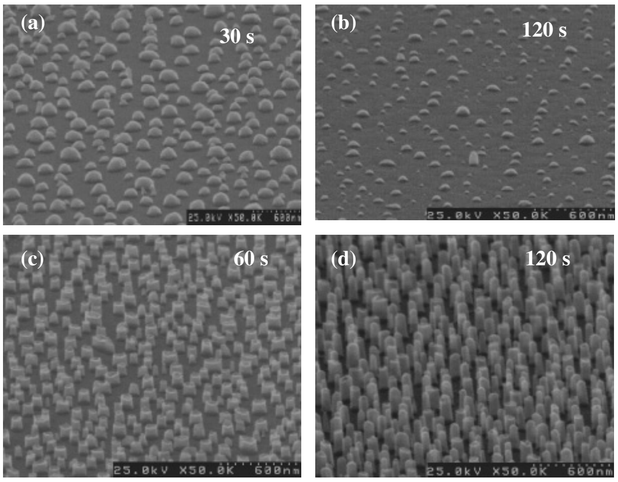

Fig. 2. SEM images of Ar plasma etching of nickel nano cluster on silicon nitride for (a) 30 s (b) 120 s. SEM images of CF_4/O_2 plasma etching of nickel nano cluster on silicon nitride for (a) 60 s (b) 120 s.

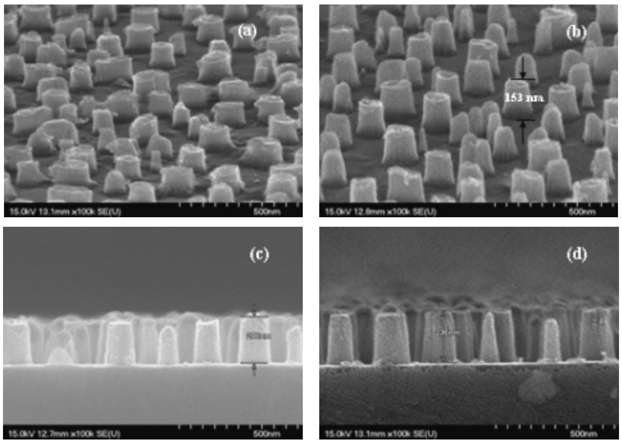

Fig. 3. SEM images of fabricated nanopillar structures on silicon nitride film using one-step etching process for etching time: (a) 90, (b) 120, (c) 150, and (d) 180 s.

Figure 4 displayed top-view and cross-sectional images of the different nanocones obtained after varying etching time of the CF_4/O_2, but keeping the etching time of Ar constant as 120 s, for the two-step process. Figures 4(a)–4(c) showed the top-view of the nanocones fabricated for the etching time of 90 s, 120 s, and 150 s respectively. Figures 4(d) and 4(e) shows the cross-section view of the structure shown in

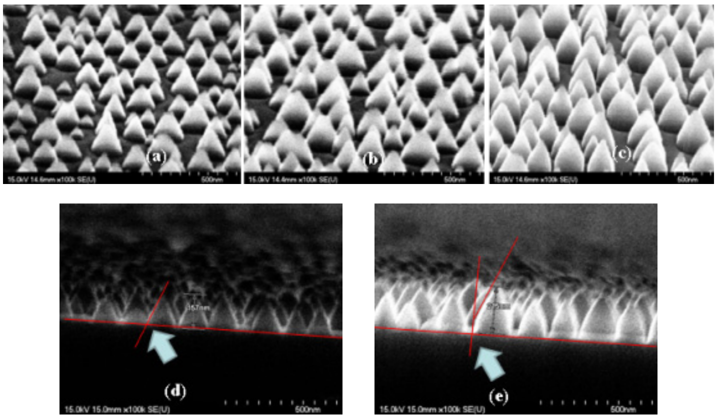

Fig. 4. (Color online) SEM images (top-view) of fabricated nanocone structures on silicon nitride film using two-step etching process for etching time: (a) 90, (b) 120, and (c) 150 s. Cross-section SEM view of the fabricated nanocone structures with etching time (d) 90 and (e) 180 s.

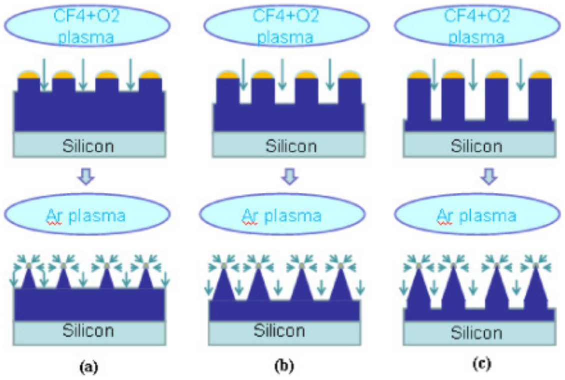

Fig. 5. (Color online) Schematic illustration of the base of the fabricated nanocones: (a) shortest etching time (b) medium etching time, and (c) longest etching time.

Figs. 4(a) and 4(c), which indicated that etched silicon nitride having a height of around 157 nm for the etching time of 90 s and around 215 nm for the etching time of 150 s, respectively. Note that in Figs. 4(d) and 4(e) the base of the nanocones were different from each other, which were clearly seen. This behavior of the nanocone base could be explained by our proposed possible mechanism as shown in Fig. 5. In the two-step etching process, first step which used the mixture of CF_4/O_2 forms the nanopillars with different heights for the different etching times as shown in Fig. 5. The longer etching time, the deeper the height of nanopillars. When we used the Ar gas in the second step of the etching process, Ar starts to etch the nickel nano clusters and preformed silicon nitride nanopillars isotropically. In the absence of a covering of nanoclusters, the etching rate of the top region of etched silicon would be slightly greater than that at the bottom.[12] For this reason, in the deeper nanopillar structures [i.e., Fig. 5(c)] the slower etching rate of the bottom region may form the longitudinal base of the nanocones.

The relations between etching time with average reflectance and structure height for nanopillars and nanocones have been shown in Figs. 6(a) and 6(b), respectively. From Fig. 6(a), it has been observed that nanocone structures shows lesser average reflectance than the nanopillar structure when we increase the etching time. Also it has been seen from Fig. 6(b) that the height of the nanocone structures higher than nanopillar structures which is clearly understood effect of the second step etching process by the Ar gas. The reflectance spectra for both nanocone and nanopillar structures with almost similar height were compared in Fig. 6(c). It has been observed that though the average reflectance for both nanocone and nanopillar structures were less than 5%, the average reflectance of nanopillar structures were better than the nanocone structure with similar height. Also it was observed that for the nanocone structures, the reflectance would be less than 6% for the shorter wavelength (i.e., from 190 to 300 nm) and longer wavelength (i.e., from 700 to 1000 nm) as well. Whereas, for nanopillar structures, the reflectance would be less than 6% for the wavelength range from 400 to 800 nm. Since both the structures could produce an average reflectance of less than 5%, which is very good for an ARC to be applied in solar cell, it is believed that silicon nitride nano structures would be very useful for replacing the DLAR coatings and can give a better or comparable performance. But, nanocone structures have been observed to provide lower average reflectance of below 6% for a longer range of heights as compared to nanopillar structures. So nanocone would be better structures to be used as silicon nitride sub-wavelength structures for solar cell applications due to the tolerance of wider heights variation of the structure.

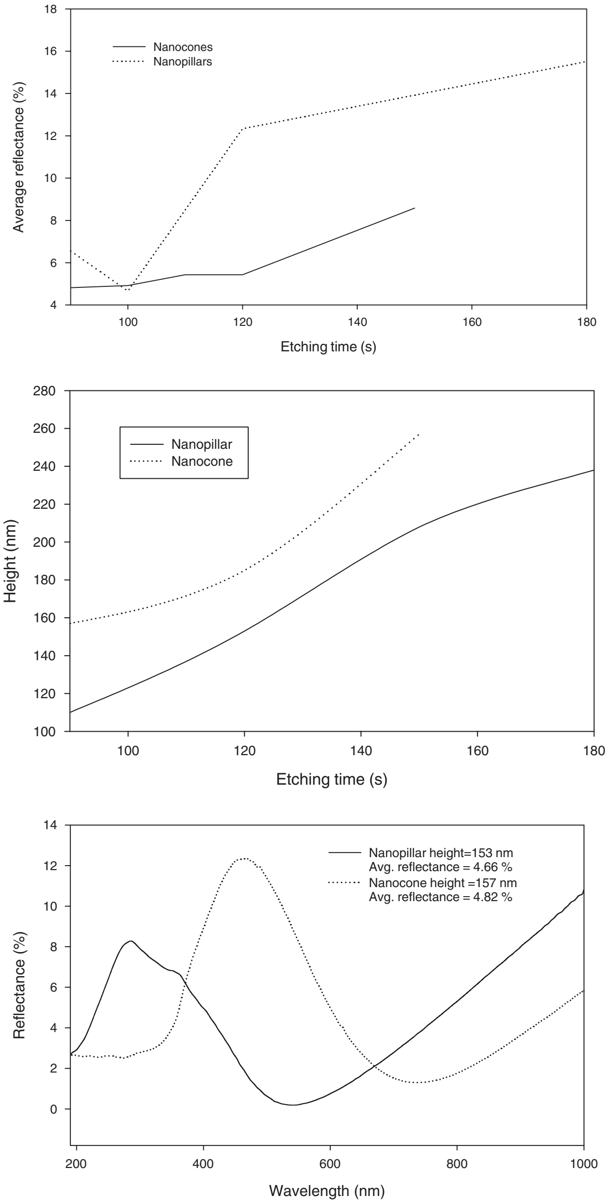

Fig. 6. Relationship between etching time with (a) average reflectance and (b) structure height for the fabricated nanocone and nanopillar structures on silicon nitride film. (c) The reflectance spectra comparison of nanocone and nanopillar structures with almost same height for the wavelength from 190 to 1000 nm.

4. Conclusions

In summary, we have developed an easy and scalable non-lithographic approach for creating nanocone and nanopillar structured antireflection coatings directly on silicon nitride using nickel nano cluster and ICP etching method for the solar cell application. The one step ICP etching process using a gas mixture of CF_4/O_2 can produce nanopillar structures and two step etching process using gas mixture of CF_4/O_2 in first step and Ar in second step can produce nanocone structures on silicon nitride film using nickel self assembled nickel nanocluster mask. The measured reflectance for both the structures shows a great promise to be used in solar cell to improve the efficiency because of its lower average reflectance of less than 5%. Nanocone structures have been observed to provide lower average reflectance of below 6% for a longer range of heights as compared to nanopillar structures. So it can be concluded that nanocones are better structures to be used as silicon nitride sub-wavelength structures for solar cell applications due to the tolerance of wider heights variation of the structure.

Acknowledgements

This work was supported in part by Taiwan National Science Council (NSC) under Contract NSC-96-2221-E-009-001-PAE, and by Motech Industries Inc. (MOTECH), Tainan, Taiwan, under a 2008-2009 grant.

1) J. A. Mazer: *Solar Cells: An Introduction to Crystalline Photovoltaic Technology* (Kluwer Academic, Boston, MA, 1997) 1st ed., p. 139.
2) S. M. Sze: *Semiconductor Devices: Physics and Technology* (Wiley, New York, 2007) 3rd ed., p. 682.
3) S. Strehlke, S. Bastide, J. Guillet, and C. Levy-Clement: Mater. Sci. Eng. B **69** (2000) 81.
4) K. Nishioka, S. Horita, K. Ohdaira, and H. Matsumura: Sol. Energy Mater. Sol. Cells **92** (2008) 919.
5) C. H. Sun, W. L. Min, N. C. Linn, and P. Jiang: Appl. Phys. Lett. **91** (2007) 231105.
6) Z. Yu, He Gao, W. Wu, H. Ge, and S. Y. Chou: J. Vac. Sci. Technol. B **21** (2003) 2874.
7) P. Lalanne and G. M. Morris: Nanotechnology **8** (1997) 53.
8) T. Ohira, T. Segawa, K. Nagai, K. Utaka, and M. Nakoi: Jpn. J. Appl. Phys. **41** (2002) 1085.
9) K. C. Sahoo, M. K. Lin, E. Y. Chang, Y. Y. Lu, C. C. Chen, J. H. Huang, and C. W. Chang: Nanoscale Res. Lett. **4** (2009) 680.
10) K. C. Sahoo, Y. Li, and E. Y. Chang: Comput. Phys. Commun. **180** (2009) 1721.
11) C. M. Hsu, S. T. Connor, M. X. Tang, and Y. Cui: Appl. Phys. Lett. **93** (2008) 133109.
12) H. Xiao: *Introduction to Semiconductor Manufacturing Technology* (Prentice Hall, Upper Saddle River, NJ, 2001).